Ion kinetics and symmetric charge-transfer collisions in low-current, diffuse (Townsend) discharges in argon and nitrogen

S. B. Radovanov,* R. J. Van Brunt, and J. K. Olthoff
Electricity Division, Electronics and Electrical Engineering Laboratory, National Institute of Standards and Technology, Gaithersburg, Maryland 20899

B. M. Jelenkovic†
Joint Institute for Laboratory Astrophysics, University of Colorado and National Institute of Standards and Technology, Boulder, Colorado 80309-0440

(Received 8 August 1994)

Translational kinetic-energy distributions of mass-selected ions have been measured in diffuse, low-current Townsend-type discharges at high electric field-to-gas density ratios (E/N) in the range of 1×10^{-18}–2×10^{-17} V m^2 (1–20 kTd). The discharges were generated in Ar and N_2 under uniform-field conditions and ion energies were measured using a cylindrical-mirror energy analyzer coupled to a quadrupole mass spectrometer. The mean ion energies determined from measured energy distributions of Ar^+ in Ar and N_2^+ in N_2 are compared with the mean energies predicted from solutions of the Boltzmann transport equation based on the assumption that symmetric resonant charge transfer is the predominant ion-neutral interaction. The results for Ar^+ and N_2^+ are consistent with predictions made using a constant (energy independent) cross section for which an effective ion temperature can be defined. However, for both ions, the measured mean energies tend to fall increasingly below the predicted values as E/N increases. The possible causes and significance of the differences between the measured and calculated mean ion energies are examined by considering collisions other than charge-transfer that can affect ion energies as well as uncertainties in the charge-transfer cross sections used in the calculations. Measurements were also made of the relative contributions from N^+ and Ar^{2+} to the ion flux. Over the E/N range of interest, N^+ accounts for less than 15% of the ion flux in nitrogen and Ar^{2+} accounts for less than 5% of the ion flux in argon.

PACS number(s): 52.40.−w

I. INTRODUCTION

The importance of resonant charge-transfer processes in determining the kinetic-energy distributions of ions in radio-frequency (rf) discharges has become evident from numerous recent investigations [1–6,8]. The results of these investigations for argon have stimulated discussion about the relative roles played by charge transfer versus other elastic and inelastic ion-neutral collisions in affecting ion energies within the discharge sheath region [7,9–11]. Charge transfer has also been invoked to explain the observed energies of positive ions in the cathode fall region of dc glow discharges [12–17].

Velocity distributions of Ar^+ in Ar have been measured by Ong and Hogan [18] in a uniform-field drift tube for electric field-to-gas density ratios (E/N) up to 3.2×10^{-19} V m^2 (320 Td). They found that the measured distributions showed increasing deviations from a Maxwellian distribution as E/N was increased. It has been shown [15,19–21] from solution of the Boltzmann equation in one dimension that if resonant charge transfer is the dominant interaction with a constant, energy independent cross section Q_{CT} then the ion-energy distribution should be of a Maxwellian form from which an effective ion "temperature" T_+ can be defined and is given by

$$T_+ = \frac{e}{kQ_{CT}}\left(\frac{E}{N}\right), \tag{1}$$

where e is the electron charge and k is the Boltzmann constant. The assumptions that lead to Eq. (1) will be examined in the next section. The corresponding ion drift velocity is given by

$$W_+ = \left(\frac{2kT_+}{\pi M}\right)^{1/2}, \tag{2}$$

where M is the ion mass.

Makabe and Shinada [22] have pointed out difficulties with the ion sampling procedures used in drift-tube experiments such as those performed by Ong and Hogan [18], which can lead to distortions in measured ion-

*Guest scientist from the Institute of Physics, P.O. Box 57, Belgrade, Yugoslavia. Present address: University of New Mexico, Department of Chemical and Nuclear Engineering, Albuquerque, NM 87131.

†Guest scientist from the Institute of Physics, P.O. Box 57, Belgrade, Yugoslavia. Present address: NIST, Time and Frequency Division, Boulder, CO 80303.

1063-651X/95/51(6)/6036(11)/$06.00

velocity distributions. Lin and Bardsley [23] had previously argued that differences between measured and calculated ion-velocity distributions are probably due to effects of discrimination in the experimental sampling. Using computer simulations, Skullerud and Holmstrom [24] have demonstrated that the velocity distribution of ions in a drift tube measured by the retarding potential difference (RPD) method will differ considerably from the distribution in the "boundary-free" transport region. This difference arises from the influence of ion absorption and reflection at the analyzer boundary and is greatest for the low-energy end of the distribution. They also argue that similar effects could distort results from drift-tube–mass-spectrometer experiments.

It has been shown from Monte Carlo simulations [25] that deviations from the Maxwellian form for ion-velocity distributions occur in cases where resonant charge transfer is not the dominant ion-atom interaction such as for K^+ transport in Ar. There have also been several reports [22,26–29] of enhancements in the high-energy tails of ion-energy distributions measured in drift tubes for cases where resonant charge transfer does not necessarily dominate. Mase and co-workers [30] have shown experimentally that at sufficiently high E/N there may not be enough collisions on average to establish the equilibrium condition required for validity of the Boltzmann transport equation. Under these conditions, the observed distributions deviate from those that apply under equilibrium conditions, e.g., a Maxwellian distribution, as manifested by an enhancement in the high-energy tail. At extremely low pressures, the ion-energy distribution in a uniform-field drift tube will assume a "beamlike" characteristic and exhibit a narrow peak at the maximum energy determined by the product of applied electric field and total drift length. This has been observed [30] for Ar^+ in Ar where, under equilibrium conditions, charge transfer is expected to dominate.

Deviations from equilibrium behavior in electron transport have been investigated under a variety of conditions and shown to occur for E/N as low as 3×10^{-19} V m^2 (300 Td) [31–34]. Less is known about the conditions under which nonequilibrium transport can be expected for ions when charge transfer is the dominant collision process.

The extent to which resonant charge transfer is the dominant ion-molecule interaction at relatively high E/N where inelastic collisions can occur for systems like Ar^+ in Ar or $N_2{}^+$ in N_2 is still debatable. Even at relatively low E/N (below 2×10^{-18} V m^2), the theoretical ion drift velocity of Ar^+ in Ar based on a charge-transfer model is higher than that determined from experiment [19,35]. The reason for this discrepancy is unclear, but suggests possible problems with the charge-transfer cross-section and/or ion-mobility measurements. It should be noted, as pointed out by Phelps and Jelenkovic [36], that the values of kT_+ that apply for cases where resonant charge transfer dominates are significantly higher than kT_{eff} calculated from drift velocities using the Wannier approximation [37,38],

$$\tfrac{3}{2}kT_{\text{eff}} \cong \tfrac{3}{2}kT + M(v_d)^2, \tag{3}$$

where T is the gas temperature and v_d is the ion drift velocity. This is seen by substituting W_+ from Eq. (2) for v_d into Eq. (3), which in the high-field limit gives

$$\frac{kT_+}{kT_{\text{eff}}} = \frac{3\pi}{4}, \tag{4}$$

where the second term on the right-hand side of Eq. (3) is assumed to dominate over the first term.

There is experimental evidence [36,39] that, at E/N greater than 10^{-17} V m^2, electronic excitation of Ar in Ar^+–Ar collisions begins to become significant. The effect of inelastic collisions involving electronic excitation on the kinetic-energy distribution of Ar^+ would likely be most evident at the high-energy tail for energies above 10 eV.

For $N_2{}^+$ in N_2, there is the possibility that inelastic collisions involving vibrational excitation will occur at energies below 10 eV [40]. There is also evidence [34] in this case of electronic excitation to the $B^2\Sigma_u^+$ state of $N_2{}^+$ at high E/N. As in the case of Ar^+ in Ar, inelastic collision processes will tend to reduce the mean ion energy below that predicted by assuming that charge transfer is the only ion-molecule interaction. The possible effect of inelastic processes on the shape of the energy distribution is still unresolved.

The relative contribution of N^+ to the ion flux for a Townsend discharge in nitrogen has been the subject of debate [34,41,42]. The transport of N^+ in N_2 will obviously not be predominantly affected by resonant charge transfer. Because of a lack of charge transfer and the fact that the momentum-transfer cross section for N^+–N_2 collisions falls considerably below that for $N_2{}^+$–N_2 collisions at energies above 1 eV [40], it can be argued that N^+ should have a higher mean energy than $N_2{}^+$. Moreover, it is known that N^+ formed by dissociative ionization processes can have kinetic energies considerably in excess of the thermal energy [43,44], and it has been noted [26] that this could have a perturbing effect on fragment-ion energy distributions measured in drift tubes, especially if a significant fraction of the observed ions are formed near the sampling location.

In the work described here, ion kinetic-energy distributions of mass-selected ions were measured from diffuse, low-pressure (Townsend) discharges in Ar and N_2 at relatively high E/N in the range of 1×10^{-18}–2×10^{-17} V m^2 (1 to 20 kTd). The purposes of this investigation are (1) to determine if there is any evidence of nonequilibrium behavior in the transport of ions and (2) to determine the extent to which ion transport is consistent with predictions based on a simplified, one-dimensional equilibrium model that includes only resonant symmetric charge transfer. The relative contributions of the minor ions N^+ and Ar^{2+} to the ion transport have also been measured. The results presented here supplant those given in our earlier preliminary report [45].

II. THEORY

In this section, the theory that leads to Eq. (1) is extended to allow for an energy-dependent charge-transfer

cross section. The basis for the theory is otherwise the same as discussed by previous authors [15,19,20]. The following assumptions are made (1) the ion motion takes place in a constant uniform electric field, (2) charge transfer is the predominant ion-neutral interaction, and (3) equilibrium conditions apply so that ion transport satisfies the one-dimensional Boltzmann transport equation. The form of the steady-state Boltzmann equation that incorporates these assumptions can be written as [20]

$$\frac{a}{N}\frac{\partial h(\vec{v})}{\partial v_z} + Q_{\rm CT}(v)vh(\vec{v}) = Q_{\rm CT}(v)\delta(v_z)\delta(v_x)\delta(v_y) \times \int\int\int h(\vec{v}')v'd^3v', \quad (5)$$

where

$$\frac{a}{N} = \frac{e}{M}\left(\frac{E}{N}\right), \quad (6)$$

$h(\vec{v})$ is the velocity distribution function, $\vec{v} = \hat{i}v_x + \hat{j}v_y + \hat{k}v_z$ is the ion velocity in the center-of-mass coordinates, and $Q_{\rm CT}(v)$ is the velocity-dependent charge-transfer cross section. This form is valid if $|v_z| \gg |v_x|, |v_y|$, where v_z is the component of ion velocity in the direction of the electric field. The velocity distribution function is, therefore, represented by a product of δ functions in directions perpendicular to z so that only the v_z dependence of $h(\vec{v})$ needs to be considered.

Because charge transfer is an interaction that effectively causes the ion to stop and then start again with zero velocity in the positive z direction, the velocity distribution function can be written as [20]

$$h(\vec{v}) = C\delta(v_x)\delta(v_y)s(v_z)g(v_z), \quad (7)$$

where C is a normalization constant and $s(v_z)$ is a step function defined such that $s(v_z) = 0$ for $v_z < 0$ and $s(v_z) = 1$ for $v_z \geq 0$. The function $g(v_z)$ satisfies the differential equation

$$\frac{a}{N}\frac{\partial g(v_z)}{\partial v_z} = Q_{\rm CT}(v_z)v_z g(v_z). \quad (8)$$

Integration of this equation gives

$$g(v_z) = C'\exp\left[-\left(\frac{a}{N}\right)^{-1}\int_0^{v_z} v_z' Q_{\rm CT}(v_z')dv_z'\right], \quad (9)$$

where C' is a normalization factor. The translational kinetic-energy distribution function $f(\varepsilon)$ is defined such that it is related to $g(v_z)$ by

$$(2M)^{-\frac{1}{2}}f(\varepsilon)d\varepsilon = g(v_z)dv_z, \quad (10)$$

where ε is the kinetic energy and $f(\varepsilon)$ is required by this definition to satisfy the normalization condition,

$$\int_0^\infty \varepsilon^{\frac{1}{2}}f(\varepsilon)d\varepsilon = 1. \quad (11)$$

If $Q_{\rm CT}$ is assumed to be independent of energy, i.e., $Q_{\rm CT} = A'$, where A' is a constant, then Eqs. (9)–(11) give

$$f_m(\varepsilon) \equiv f(\varepsilon) = 2(\pi)^{-1/2}\left(\frac{eE}{A'N}\right)^{-3/2} \times \exp\left[-\varepsilon\left(\frac{eE}{A'N}\right)^{-1}\right], \quad (12)$$

which has a Maxwellian form that yields an effective ion temperature given by Eq. (1). This distribution is denoted by $f_m(\varepsilon)$ and is referred to here as the "Maxwellian approximation."

If $Q_{\rm CT}$ has an energy dependence of the form

$$Q_{\rm CT}(\varepsilon) = A\varepsilon^{-\beta}, \quad (13)$$

where A and β are constants, then we obtain

$$f_b(\varepsilon) \equiv f(\varepsilon) = C'\exp\left[-\frac{A}{e(E/N)}\left(\frac{\varepsilon^{1-\beta}}{1-\beta}\right)\right]. \quad (14)$$

The normalization factor C' is obtained using Eq. (11). In this case, the distribution does not have a Maxwellian form, and therefore, a "temperature" cannot be defined. The function given by Eq. (14) is referred to here as the "Boltzmann approximation" and is denoted by $f_b(\varepsilon)$. Note that

$$\lim_{\beta\to 0}\left[\lim_{A\to A'} f_b(\varepsilon)\right] = f_m(\varepsilon), \quad (15)$$

as required. Of particular relevance to the analysis of the data on energy distributions presented in this work are the fractional differences in the mean relative slopes of $\ln[f_b(\varepsilon)]$ and $\ln[f_m(\varepsilon)]$, namely,

$$\Delta_s = \frac{\left|\left\langle\frac{d\ln[f_b(\varepsilon)]}{d\varepsilon}\right\rangle - \left\langle\frac{d\ln[f_m(\varepsilon)]}{d\varepsilon}\right\rangle\right|}{\left\langle\frac{d\ln[f_m(\varepsilon)]}{d\varepsilon}\right\rangle} \simeq \frac{|A\langle\varepsilon\rangle^{-\beta} - A'|}{A'}, \quad (16)$$

where $\langle\varepsilon\rangle$ is the mean ion energy.

Figure 1 shows the total resonant symmetric charge-

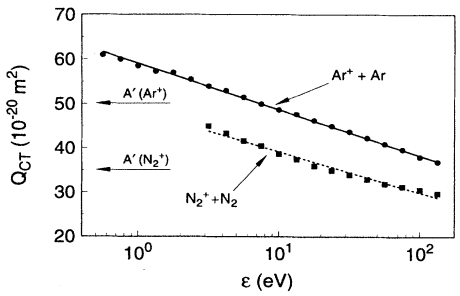

FIG. 1. Symmetric charge-transfer cross sections for $Ar^+ - Ar$ and $N_2^+ - N_2$ from Phelps (Ref. [40]) and the fits used in the present analysis given by the solid and dashed lines. The parameters obtained from fitting the data are given in Table I. The horizontal arrows indicate the constant values for the cross sections used in the Maxwellian approximation.

TABLE I. Values for A', A, and β used to represent the two forms of the charge-transfer cross-sections in units of 10^{-20} m^2 for Ar^+-Ar and $N_2{}^+-N_2$ collisions. Also shown are values of Δ_s calculated using Eq. (16) for the different indicated values of $\langle\varepsilon\rangle$.

Reaction	A' (10^{-20} m^2)	A (eV$^\beta \times 10^{-20}$ m^2)	β	Δ_s		
				$\langle\varepsilon\rangle = 5$ eV	$\langle\varepsilon\rangle = 10$ eV	$\langle\varepsilon\rangle = 20$ eV
$Ar^+ + Ar$	49.6	62.23	0.105	0.059	0.015	0.084
$N_2{}^+ + N_2$	35.7	50.36	0.111	0.180	0.092	0.012

transfer data for Ar^+-Ar and $N_2{}^+-N_2$ collisions that have been used in the present analysis together with corresponding fits to the data of the form indicated by Eq. (13). The cross-section data are those recommended by Phelps [40], and were derived from various sources [46–49]. The horizontal arrows indicate the values for A' (constant Q_{CT}) that were assumed for the Maxwellian approximation. The values for A', A, and β used in the analysis discussed here are listed in Table I together with values for Δ_s that were calculated for the indicated values of the mean ion energy. The mean ion energies were selected to lie within the ranges corresponding to the values for E/N covered in the experiments described here. It is seen from the Δ_s values that the slopes of $\ln[f_b(\varepsilon)]$ and $\ln[f_m(\varepsilon)]$ versus ε curves differ by less than 10% over most of the energy range of interest. As shown below, fits to the experimental data using both $f_b(\varepsilon)$ and $f_m(\varepsilon)$ typically yield the same results for mean ion energy to within the scatter and uncertainties in the data, i.e., it is difficult to distinguish between the two forms for the distribution from the experimental data and the effect of including the energy dependence for the charge-transfer cross section is of little or no consequence for either Ar^+ in Ar or $N_2{}^+$ in N_2 when E/N is within the range considered here. In general, it can be expected that the mean ion energies calculated using measured energy distributions will be insensitive to minor changes in the distribution profiles.

III. EXPERIMENT

The experimental setup is shown diagrammatically in Fig. 2. The configuration of the discharge cell is similar to that used in earlier work [50]. It consisted of two parallel circular stainless-steel electrodes 4.2 cm in diameter separated by a distance of 1.4 cm. The discharge occurs between the electrodes that are surrounded by a cylindrical quartz insulator as shown in the figure. The ions were sampled through a 0.1-mm-diameter aperture in the cathode. The high voltage was applied to the anode and the cathode was connected to ground through a 27-kΩ resistor. The electrode separation is large enough to insure that $d \gg \lambda$, where λ is the mean-free ion path, and small enough to avoid significant perturbation of the electric field on the axis defined by the sampling aperture due to charging of the quartz surface. The results are insensitive to small variations of d around the value selected.

The gas pressure in the discharge cell was measured

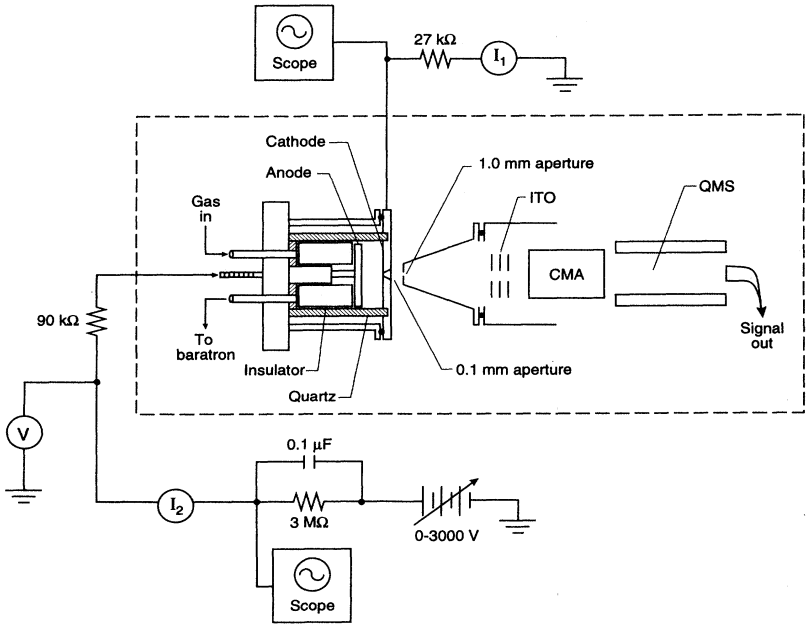

FIG. 2. Experimental arrangement. Shown are the discharge cell, external circuit, ion-transfer optics (ITO), cylindrical mirror energy selector (CMA), and the quadrupole mass spectrometer (QMS). The baratron is an electronic capacitance manometer to measure the gas pressure in the discharge volume. The components within the dashed box are contained in the vacuum system.

with a baratron and was maintained at a constant value to within ±0.13 Pa in the range of 17.0–45.0 Pa. The gas number density N was calculated from the pressure using the ideal gas law. The electric-field strength was assumed to be uniform and given by V/d, where V is the voltage measured across the electrodes. The maximum uncertainties in E/N result primarily from drift or fluctuations in the gas pressure and are estimated to range from $\pm 4.0 \times 10^{-21}$ V m^2 at low E/N ($\sim 2 \times 10^{-18}$ V m^2) to $\pm 1.0 \times 10^{-19}$ V m^2 at high E/N ($\sim 20 \times 10^{-18}$ V m^2).

Kinetic-energy distributions of specific, mass-selected ions were measured using a differentially pumped cylindrical mirror analyzer (CMA) coupled to a quadrupole mass spectrometer (QMS). The configuration is similar to that used recently by Kumar and Ghosh [16] to measure ion-energy distributions from glow discharges in nitrogen. The CMA-QMS system used in the present work is identical to that described by Olthoff and co-workers [4] for measurement of ions from rf glow discharges in argon. In the present work, measurements were made both with and without the stainless-steel sampling cone. This is the cone with a 1.0-mm aperture shown in Fig. 2. Measurements were also made both with the lens elements of the ion-transfer optics (ITO) grounded to the same potential as the cathode and with the ITO operated in the normal einzel lens mode. With the sampling cone in place, tests were performed to determine the effect of varying the cone-to-cathode spacing from 4 to 10 mm. It was found that all of the operating configurations yielded results that agreed to within the estimated uncertainties discussed below, thus indicating that effects of angular spread in ion trajectories due to nonaxial velocity components did not significantly perturb the measured "axial" energy distributions.

Ion kinetic-energy distributions were measured under conditions where the mass spectrometer was tuned to a specific mass-to-charge ratio while the potential difference between the CMA and ITO was scanned so that the observed ions always passed through the analyzer with a fixed energy of 20 eV. The energy resolution of the CMA was maintained at 2.0 eV (full width at half maximum) over the entire energy range scanned. Using a K^+ ion beam, it was determined that the transmission of the CMA-QMS was constant up to an ion energy of about 150 eV. Above this energy there was a decrease in the transmission due to limitations on the operating voltages of the QMS. The drop off in ion intensity seen in our earlier preliminary results [45] at about 50 eV could not be reproduced in subsequent measurements, and was most likely an instrumental effect due to misalignment and/or improper tracking of the mass-spectrometer operating voltage with ion energy.

During operation of the discharge, the currents I_1 and I_2, respectively, to the cathode and anode, were measured simultaneously. When an insulator was inserted behind the anode (see Fig. 2), it was found that $I_1/I_2 = 1.0$ over the entire E/N range that was investigated for both gases. When the insulator was removed, it was found that I_2 could become significantly greater than I_1 at E/N values greater than 10^{-17} V m^2 (10 kTd) due to the possible occurrence of discharges on the "back side" of the anode. The energy distributions obtained when I_2 exceeded I_1 were, nevertheless, in agreement with those obtained when the insulator was present and $I_1 = I_2$.

The discharge was operated in the Townsend regime where the current is nearly independent of the measured gap voltage [51]. The voltages in this case correspond to points on the "left-hand" side of the Paschen minimum [36,52,53]. Shown in Fig. 3 is an example of a Paschen curve for argon determined for the experimental conditions described here. Indicated are the E/N values of 17.4×10^{-18} V m^2 and 2.3×10^{-18} V m^2 at which some of the results reported below were obtained. The measured ion-energy distributions were insensitive to discharge current selected within the "flat" part of the characteristic voltage-current curve corresponding to the Townsend discharge region. The ion signal levels increased approximately linearly with current within this region as expected. The small decrease of current with voltage across the gap for Townsend discharges in pure argon reported in some earlier works [54,55] was not always evident for the conditions used in the present experiments. The upper limit on the discharge current that could be used was determined by the onset of discharge instabilities manifested by the occurrence of large current pulses or oscillations that are the prelude to the formation of a normal glow discharge [51,56]. This oscillatory or pulsating behavior has been reported previously and is known to be influenced by the configuration of the external circuit [57]. It is worth noting that the ion-energy distributions measured under glow discharge conditions differed considerably from those reported here for a diffuse Townsend discharge. For all the measurements reported in this work, the discharge current was between 2.0 and 3.0 μA for argon and between 5.0 and 8.0 μA for nitrogen.

Both the argon and nitrogen experiments were performed using high purity gases (99.999% purity). It was found, nevertheless, that effects of cell contaminants, particularly water vapor desorbing from the insulator, could be observed during the first few hours of discharge operation. The presence of H_2O was periodically monitored by

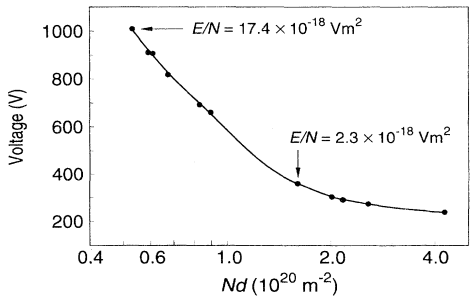

FIG. 3. Example of a Paschen curve experimentally determined for argon using the apparatus shown in Fig. 2. Indicated are the values $E/N = 17.4 \times 10^{-18}$ V m^2 and $E/N = 2.3 \times 10^{-18}$ V m^2 that were obtained, respectively, at pressures of 17.3 and 44.7 Pa.

tuning the QMS to detect ions at mass-to-charge ratios of 17 u and 18 u, corresponding, respectively, to OH^+ and H_2O^+. In the case of nitrogen, the presence of water vapor caused a large signal (sometimes comparable in intensity to that for N_2^+) to appear at a mass-to-charge ratio of 29 u corresponding to the ion N_2H^+. This ion is known [58–60] to be formed by the fast reaction,

$$N_2^+ + H_2O \rightarrow N_2H^+ + OH. \quad (17)$$

To avoid possible effects of contaminants such as H_2O, measurements of ion-energy distributions were not performed until the ion signals associated with contaminants, e.g., N_2H^+ and OH^+, reached levels that were at least an order of magnitude below those for the ions of interest, e.g., Ar^+ and N_2^+.

The surfaces of the stainless-steel electrodes were polished before they were inserted into the discharge cell. It was found, nevertheless, that, except for low-energy discrimination effects discussed in the next section, the measured energy distributions were not noticeably affected by the condition of the electrode surfaces.

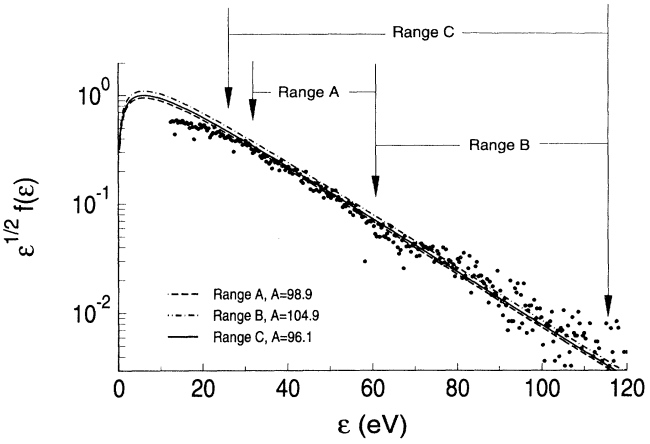

FIG. 5. Measured ion-energy distributions for $N_2^+ - N_2$ at $E/N = 4.8 \times 10^{-18}$ V m^2. Indicated are fits to the data using the "Boltzmann" form for three different energy ranges and the corresponding values obtained for the cross-section parameter A in units of (eV)$^\beta \times 10^{-20}$ m^2. The parameter β was kept at a constant value of 0.111.

IV. ANALYSIS AND RESULTS

Examples of measured ion-energy distributions are shown in Figs. 4 and 5, respectively, for Ar^+ in Ar and N_2^+ in N_2. No data are shown for energies below 10 eV where it was found from independent tests at low E/N using a drift tube that there were severe discrimination effects [61]. In addition to problems noted by others [22–24], there is evidence that the ion discrimination at low energies is also due in part to effects of surface charging at or near the sampling apertures [4].

Plotted in Figs. 4 and 5 are the normalized distributions $\varepsilon^{1/2} f(\varepsilon)$ versus ε. The distributions have been arbitrarily normalized to their projected maximum values. All of the measured distributions have been fitted to the forms $f_m(\varepsilon)$ and $f_b(\varepsilon)$ given by Eqs. (12) and (14). As examples, the lines shown in Fig. 4 correspond to $\varepsilon^{1/2} f_m(\varepsilon)$ and those in Fig. 5 to $\varepsilon^{1/2} f_b(\varepsilon)$. The three different lines that are shown correspond to least-squares fits using the three different energy ranges (A, B, and C) shown in the figures. The normalization of each fit has been made slightly different to displace the lines so that they can be distinguished easily. The data selected for fitting were restricted to the range 120 eV $\geq \varepsilon \geq$ 20 eV where there was no evidence of significant distortion due to effects of energy-dependent transmission or discrimination. In making fits to the experimental data, A' and A in Eqs. (12) and (14) were treated as free parameters.

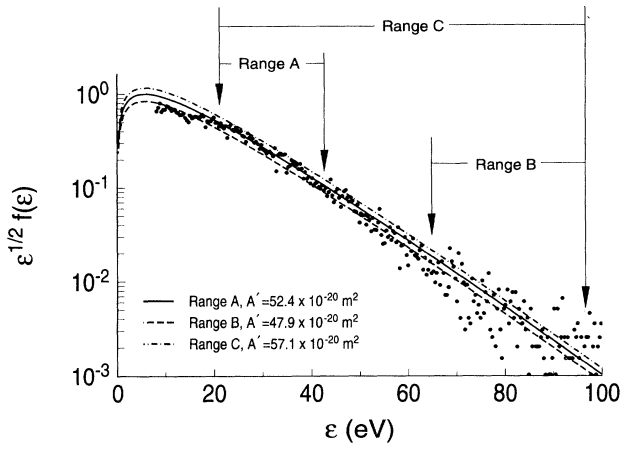

FIG. 4. Measured ion-energy distributions for $Ar^+ - Ar$ at $E/N = 5.95 \times 10^{-18}$ V m^2. Indicated are fits to the data using the "Maxwellian" form for three different energy ranges and the corresponding values obtained for the cross-section parameter A' in units of 10^{-20} m^2.

From the fitted forms of the kinetic-energy distributions, the mean ion energies were computed using

$$\langle \varepsilon \rangle = \int_0^\infty \varepsilon^{3/2} f_x(\varepsilon) d\varepsilon, \quad (18)$$

where $x = m$ or b, depending on which form was used. The mean energies experimentally determined by this method were compared with those predicted using the $f_m(\varepsilon)$ and $f_b(\varepsilon)$ obtained with the values for A', A, and β given in Table I from fits to the charge-transfer cross-section data (see Fig. 1). The analysis used here to determine experimental mean energies relies on an accurate determination of the high-energy tail of the distribution and the assumption that it can be extrapolated to low energies using one or both of the forms corresponding to $f_m(\varepsilon)$ and $f_b(\varepsilon)$. We would argue that, given the limited understanding of low-energy discrimination effects, the analysis method employed here is the best that can be considered at the present time.

The results from the analysis of the measured energy distributions to determine mean ion energies are shown in Figs. 6 and 7, respectively, for argon and nitrogen. In addition to the mean energies for N_2^+, Fig. 7 shows mean energies for N^+ estimated from the experimental data assuming a Maxwellian form for the energy distributions. The dot-dash line is simply a linear fit to the N^+ data and has no theoretical significance. The open symbols in both Figs. 6 and 7 denote data taken under conditions where (1) the insulator was inserted behind the anode, (2) the sampling cone was removed, and (3) all ITO elements were grounded. The closed symbols correspond to the opposite set of conditions where (1) the insulator was removed, (2) the sampling cone was inserted, and (3) the ITO was used to focus ions into the energy analyzer. The ion signal levels at a given E/N were generally higher for the latter set of conditions.

The figures show predicted and experimentally determined mean energies obtained using both the Maxwellian and Boltzmann approximations. The error bars correspond to the uncertainties associated primarily with variations in the results determined from selecting different energy ranges for fitting to the assumed forms of the distributions (see Figs. 4 and 5). Each data point corresponds to a value obtained by taking the full energy range (range C in Figs. 4 and 5). The error limits correspond to the high- and low-energy extremes, e.g., ranges A and B in Figs. 4 and 5. These uncertainties are an indication of how well the measured distributions can be represented by the assumed forms $f_b(\varepsilon)$ and $f_m(\varepsilon)$. The deviations from these forms are relatively small, but tend to increase at the high ends of the E/N ranges considered.

Other sources of uncertainty were generally of much lower significance than those associated with the fitting of the data. The largest of these other sources is that arising from uncertainties in the ion-energy scale. In our earlier work [4], energy shifts as large as 3.5 eV were noted. These shifts were attributed to charge buildup on the inner surface of the sampling cone. In the present work, the uncertainties in the energy scale due to shifts

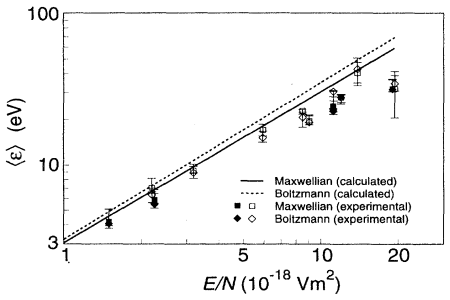

FIG. 6. Comparison of the predicted and experimentally determined mean ion energies for Ar^+-Ar versus E/N obtained using both the Maxwellian and Boltzmann approximations. The open and closed symbols correspond to measurements made with different ion-transfer conditions used for operation of the CMA-QMS as discussed in the text.

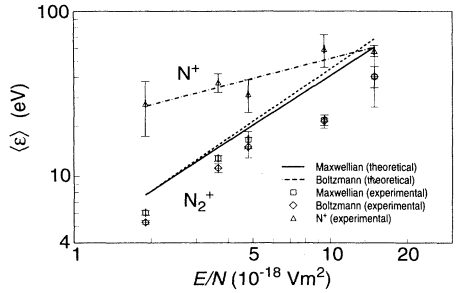

FIG. 7. Comparison of the predicted and experimentally determined mean ion energies for $N_2^+-N_2$ versus E/N obtained using both the Maxwellian and Boltzmann approximations. Also shown are the estimated mean energies for N^+ and the corresponding fit to these data given by the dot-dash line.

are estimated to be less than ± 1.0 eV. This uncertainty has a relatively small effect on the calculated mean energy. For example, an analysis of the Ar^+ data at $E/N = 3.2 \times 10^{-18}$ V m^2 (3.2 kTd) showed that an assumed extreme ± 3.0 eV variation in the energy scale corresponded to a ± 0.1 eV change in $\langle\varepsilon\rangle$ calculated using the Maxwellian approximation. This is much smaller than the uncertainty implied by the error bars in Fig. 6. The relatively small uncertainty due to energy shifts is a consequence of the fact that the slopes of the $\ln[f_m(\varepsilon)]$ (or $\ln[f_b(\varepsilon)]$) versus ε curves that primarily determine $\langle\varepsilon\rangle$ are not sensitive to small energy shifts.

Another relatively minor source of systematic error that could affect the scatter in the data is that associated with drift in the discharge conditions that define E/N, e.g., gas pressure and applied voltage. However, the results obtained using different operating configurations mentioned above generally tend to agree to within the uncertainties associated with fitting of the data. For Ar^+ in Ar, the mean energies determined from both experimental data and theory using $f_m(\varepsilon)$ tend to fall systematically below those determined using $f_b(\varepsilon)$. Independent of the assumed form for the energy distribution, the experimental mean energies for Ar^+ are lower than predicted, and this deviation from prediction is greatest and most significant at higher E/N (greater than 6.0×10^{-18} V m^2). Despite the difficulties mentioned in the preceding section, the results for Ar^+ are consistent with those given in our earlier primary work [45] for $E/N > 10^{-18}$ V m^2.

The experimental mean energies obtained for N_2^+ in N_2 are seen in Fig. 7 to fall consistently below the predicted values throughout the E/N range considered. There are no significant differences between the results for N_2^+ obtained using the two different distributions. The results for N^+ show more uncertainty than those for N_2^+ due to the lower N^+ signal levels.

The relative contribution of N^+ to the ion flux hitting the cathode was estimated from the data using the assumption of Maxwellian distributions in the formula

$$\frac{I_{N^+}}{I_{N_2^+}} = \frac{\sum_{i=a}^{b} I_{N^+}(\varepsilon_i) \int_{\varepsilon_a}^{\varepsilon_b} \varepsilon^{1/2} f_m^{N_2^+}(\varepsilon, E/N) d\varepsilon}{\sum_{i=a}^{b} I_{N_2^+}(\varepsilon_i) \int_{\varepsilon_a}^{\varepsilon_b} \varepsilon^{1/2} f_m^{N^+}(\varepsilon, E/N) d\varepsilon}, \quad (19)$$

where the summations and integrations are performed over an energy interval $\varepsilon_b \geq \varepsilon \geq \varepsilon_a$ in which discrimination effects are not significant and $I_{N^+}(\varepsilon_i)$ and $I_{N_2^+}(\varepsilon_i)$ are the recorded currents (or ion counts) at equal numbers of discrete nominal energy values ε_i. This method of estimation avoids the issue of possible differences in the levels of low-energy discrimination for the two types of ions. Maxwellian distributions determined from fits to the experimental data were used in Eq. (19). The results of this estimate are compared in Table II for different E/N with a cruder estimate from the raw data given by

$$\left(\frac{I_{N^+}}{I_{N_2^+}}\right)_e = \frac{\sum_{i=1}^{n} I_{N^+}(\varepsilon_i)}{\sum_{i=1}^{n} I_{N_2^+}(\varepsilon_i)}, \quad (20)$$

where n is the total number of recorded data points. The results from the two methods of estimation are in reasonable agreement, thus suggesting levels of discrimination that are nearly equal for the ions N^+ and N_2^+. It is seen that the relative contribution of N^+ increases with E/N, but is always less than 15% of the N_2^+ flux. In the case of argon, an estimate was also made of the relative Ar^{2+} flux. Because the poor quality of the Ar^{2+} data did not permit a reasonable determination of the energy distribution function, the estimates were only made using the raw data, i.e.,

$$\left(\frac{I_{Ar^{2+}}}{I_{Ar^+}}\right)_e = \frac{\sum_{i=1}^{n} I_{Ar^{2+}}(\varepsilon_i)}{\sum_{i=1}^{n} I_{Ar^+}(\varepsilon_i)}. \quad (21)$$

The results of these estimates for different E/N are given in Table III. It is seen that the relative contribution of Ar^{2+} to the ion flux is always less than 5% of that from Ar^+. The present results for the Ar^{2+}/Ar^+ intensity ratio are consistent with those given in our earlier preliminary report [45].

Unlike the results from glow discharges [4,5], there was no evidence of significant dimer (Ar_2^+) formation. Conditions in a high E/N Townsend discharge considered here are not expected to be favorable for the production of Ar_2^+. The formation of this ion requires low-energy collisional stabilization and is, therefore, most likely to occur in the low-field regions of a discharge [4,5,62,63].

TABLE II. The relative intensity ratios of N^+ to N_2^+ estimated by the two methods discussed in the text.

E/N (10^{-18} V m^2)	$I_{N^+}/I_{N_2^+}$	$(I_{N^+}/I_{N_2^+})_e$
2.4	0.012	0.010
3.7	0.064	0.062
4.8	0.043	0.049
9.5	0.096	0.107
14.6	0.134	0.124
19.0		0.140

TABLE III. The relative intensity ratio of Ar^{2+} to Ar^+.

E/N (10^{-18} V m^2)	$(I_{Ar^{2+}}/I_{Ar^+})$
1.5	0.019
1.7	0.020
2.2	0.049
6.0	0.020
7.5	0.010
13.9	0.050
15.4	0.020
19.4	0.030

V. DISCUSSION AND CONCLUSIONS

A. Argon

For E/N in the range of 1×10^{-18}–20×10^{-18} V m^2, the measured Ar^+ kinetic-energy distributions in Ar are consistent with equilibrium-type distributions derived from solutions of the one-dimension Boltzmann transport equation. The differences between the distributions obtained with and without an assumed energy dependence of the predominant symmetric resonant charge-transfer cross section are not significant and are generally smaller than, or comparable to, the uncertainties that arise from choosing different energy ranges to fit the data. The energy distributions appear to be adequately approximated by a Maxwellian form which justifies the assignment of an effective ion temperature used in earlier work, to model discharges in argon at high E/N [36,39].

It was found, however, that the mean ion energy tends to fall systematically below that which is predicted assuming that charge transfer is the only ion-neutral interaction. The difference between predicted and experimentally determined mean ion energies increases with increasing E/N, thus suggesting that the effects of energy loss resulting from collisions other than charge transfer are influencing the distribution of ion energies.

In considering possible energy loss by collisions other than resonant charge transfer, it should be noted, as pointed out in a recent communication by Phelps [9], that momentum transfer in elastic ion-atom collisions cannot be treated as distinct from momentum transfer due to symmetric charge transfer. Symmetric charge transfer is often observationally treated as equivalent to a process in which ions are elastically scattered in the backward direction (through 180°); although theoretically it necessarily involves an electron-transfer process in order for it to occur with significant probability. The theory [47,64–66] shows that symmetric charge transfer occurs in approximately half of the elastic collisions of the ions

with like neutral species. It can, therefore, be argued that momentum transfer associated with forward elastic scattering cannot be a significant mechanism for energy loss during ion transport.

Energy losses due to the spin exchange process,

$$Ar^+(^2P_{\frac{3}{2}}) + Ar(^1S_0) \rightarrow Ar(^1S_0) + Ar^+(^2P_{\frac{1}{2}}) \quad (22)$$

are also possible. However, the translational energy loss in such collisions is small (less than 0.2 eV) and the cross section is significant only at energies above about 10 eV [63,67–69]. It is unlikely, therefore, that this process is responsible for a major energy reduction in ion transport.

Significant energy loss per collision can occur in cases where there is electronic excitation or ionization. Evidence of electronic excitation from Townsend discharges in argon at relatively high E/N has been reported in earlier work [36,39]. The rates for ionization and excitation leading to ultraviolet (UV) emissions from ion-atom collisions in argon have been estimated here using cross sections recommended by Phelps [40] and both the predicted and experimentally determined ion-energy distribution functions. The ratio of these excitation-ionization rates to the charge-transfer rates were calculated using

$$\frac{R_{UV+e}}{R_{CT}} = \frac{\int_0^\infty [Q_{UV}(\varepsilon) + Q_e(\varepsilon)] f_b(\varepsilon, E/N)\varepsilon d\varepsilon}{\int_0^\infty Q_{CT}(\varepsilon) f_b(\varepsilon, E/N)\varepsilon d\varepsilon}, \quad (23)$$

where $Q_{UV}(\varepsilon)$ and $Q_e(\varepsilon)$ are, respectively, the cross sections for UV excitation and ionization. An upper limit on the relative energy loss rates was also estimated using

$$L = \frac{\langle \Delta\varepsilon_{UV+e} \rangle}{\langle \Delta\varepsilon_{CT} \rangle} \frac{R_{UV+e}}{R_{CT}}, \quad (24)$$

where $\langle \Delta\varepsilon_{UV+e} \rangle$ and $\langle \Delta\varepsilon_{CT} \rangle$ are, respectively, the mean effective energy losses due to electronic excitation and charge transfer. A reasonable upper limit can be calculated by letting $\langle \Delta\varepsilon_{UV+e} \rangle$ assume the value 15.75 eV corresponding to the ionization potential of argon.

Table IV lists the values that were obtained for the ratios given by Eqs. (23) and (24). It is seen that the ratio of the rate of UV excitation plus ionization to the rate for charge transfer increases by about a factor of 4 as E/N is increased from 2.2 to 19.4×10^{-18} V m^2, independent of whether the predicted or experimentally determined energy distribution functions are used. However, the rate of UV excitation plus ionization is always less than 7% of that for charge transfer. The maximum energy loss rate due to electronic excitation is less than 4% of that for charge transfer at all E/N. There is, therefore, reason to doubt that the magnitude of the differences between the predicted and measured mean Ar^+ energies at high E/N seen in Fig. 4 are consistent with the ratios of rates determined from Eqs. (23) and (24).

TABLE IV. Calculated ratios of the rate coefficients for UV excitation plus ionization to that for symmetric charge transfer in the case of Ar^+ transport in Ar at different E/N. The calculations were performed using both the predicted and experimentally determined Ar^+ energy distribution functions $f_b(\varepsilon, E/N)$. Also shown are the corresponding calculated "maximum" ratios in the energy loss rates (L).

E/N (10^{-18} V m^2)	R_{UV+e}/R_{CT} (experiment)	R_{UV+e}/R_{CT} (theory)	L (theory)
2.2	0.015	0.016	0.040
5.95	0.038	0.040	0.042
8.50	0.045	0.048	0.037
13.9	0.059	0.060	0.022
19.4	0.053	0.067	0.031

It should be noted that most of the discrepancy between the predicted and experimentally determined mean ion energies can be removed by making an 18% increase in the total charge-transfer cross section at all energies in the range considered (see Fig. 1). It is difficult to know if this is a reasonable adjustment, but it is conceivable that at least part of the difference between the measured and predicted results can be accounted for by uncertainties in the assumed cross section. In arriving at a recommended cross section for Ar^+–Ar charge transfer, Phelps [40] argued that adjustments of more than 20% should be made in the cross-section values derived from measured differential scattering cross sections for energies below 15 eV [70,71].

The results shown in Fig. 6, when extrapolated to higher E/N, appear to be inconsistent with preliminary results [45] for $E/N \geq 2.0 \times 10^{-17}$ V m^2 using the retarding potential difference (RPD) method with a similar discharge cell. The RPD results tend to yield mean ion energies that are higher than predicted from the Maxwellian approximation, i.e., from Eq. (1); whereas the present results are, if anything, lower than predictions. It should be noted, however, that the energy distributions determined by the RPD method do not conform to the Maxwellian approximation, and show evidence of deviations from equilibrium behavior. Similar deviations from equilibrium behavior were evident from RPD results obtained from Ne^+–Ne in Townsend discharges at high E/N [72]. A disadvantage of the RPD method is that the identity of the ions observed is unknown. The energy distributions determined by this method could be affected by contributions from other ions such as Ar^{2+}. However, the results given in Table III indicate that Ar^{2+} is a minor ion, and its relative contribution to the ion flux does not increase significantly with E/N up to 2.0×10^{-17} V m^2 (20 kTd).

B. Nitrogen

As in the case of Ar^+ in Ar, the measured kinetic-energy distributions of N_2^+ in N_2 are consistent with equilibrium distributions derived from solutions of the one-dimensional Boltzmann transport equation. One is again justified in defining an effective ion temperature for N_2^+ within the E/N range of $1.0–20.0 \times 10^{-18}$ V m^2. Also, like Ar^+ in Ar, the mean energies determined from the measured distributions tend to fall below the predicted values at all E/N. It is possible that at least part of the difference between the measured and predicted mean energies results from the effect of vibra-

tional excitation, which has a relatively low threshold energy (less than 0.7 eV). Shown in Table V are the calculated ratios of the vibrational-excitation-to-charge-transfer rates (R_{VIB}/R_{CT}) at different E/N. These ratios were calculated using a relationship similar to Eq. (23), with the vibrational excitation cross sections tabulated by Phelps [40]. The calculated ratios lie within the range of 0.116 ± 0.003 and show no substantial increase with E/N. Estimates of L for vibrational excitation yield values that are less than 0.03 at all E/N.

Although energy loss by electronic excitation can be inferred from previous reports [34], this mechanism is not expected to be any more effective in reducing the mean ion energy than vibrational excitation for the E/N range considered here. It can be inferred from the above estimates that the contributions from inelastic collisions should not reduce the mean ion energies significantly below those predicted assuming symmetric charge transfer is the only process that can occur. It is again possible that part of the discrepancy between the predicted and measured mean energies for N_2^+ is a consequence of uncertainties or errors in the charge-transfer cross section. However, we caution against using the results reported here to "correct" the charge-transfer cross section without performing a more complete analysis of ion transport, e.g., based on a numerical solution of the Boltzmann transport equation, which takes into account all relevant collisional excitation processes.

The results listed in Table II indicate that the relative N^+ flux increases from 1% of the N_2^+ flux at $E/N = 2.4\times10^{-18}$ V m^2 to 14% of the N_2^+ flux at $E/N = 19.0\times10^{-18}$ V m^2. This trend is expected because the mean electron energy in the discharge will increase with E/N causing an increase in the rate for dissociative ionization [43] leading to N^+ formation. Although it is possible that N^+ is also formed by ion-molecule collisions, it is presumed here that this mechanism makes only a minor contribution compared with electron-impact processes.

TABLE V. Calculated ratios of the rate coefficients for vibrational excitation to that for symmetric charge transfer in the case of N_2^+ transport in N_2 at different E/N. The calculations were performed using only the experimentally determined N_2^+ energy distribution functions $f_b(\varepsilon, E/N)$.

E/N (10^{-18} V m^2)	R_{VIB}/R_{CT}
2.4	0.119
3.7	0.117
4.8	0.118
9.5	0.114
14.6	0.114

The mean energies for N^+ are significantly higher than those for N_2^+, and the difference between the mean energies of these two ions is greatest at the lowest E/N. Higher mean energies for N^+ can be expected because symmetric charge transfer is not a dominant ion-molecule interaction in this case. Moreover, the momentum-transfer cross section for $N^+ - N_2^+$ is markedly below that for $N_2^+ - N_2$ over the kinetic-energy region of relevance here [40]. Some of the measured N^+ energy distributions exhibited evidence of deviations from Maxwellian behavior in the high-energy tails. However, the data obtained from the present experiment had too much scatter and lack of reproducibility at high energies (> 100 eV) to permit reliable estimates of the deviations from equilibrium behavior. In the case of N^+ transport in N_2, it is clear that much more experimental and theoretical work is required.

ACKNOWLEDGMENTS

The authors are grateful for valuable suggestions and comments offerred by A. V. Phelps and Z. Petrović.

[1] C. Wild and P. Koidl, Appl. Phys. Lett. **54**, 505 (1989); J. Appl. Phys. **69**, 2909 (1991).
[2] A. Manenschijn and W. J. Goedheer, J. Appl. Phys. **69**, 2923 (1991).
[3] J. Janes and C. Huth, J. Vac. Sci. Tech. A **10**, 3522 (1992).
[4] J. K. Olthoff, R. J. Van Brunt, and S. B. Radovanov, J. Appl. Phys. **72**, 4566 (1992).
[5] J. K. Olthoff, R. J. Van Brunt, S. B. Radovanov, J. A. Rees, and R. Surowiec, J. Appl. Phys. **75**, 115 (1994).
[6] J. Liu, G. L. Huppert, and H. H. Sawin, J. Appl. Phys. **68**, 3916 (1990).
[7] P. W. May, D. Field, and D. F. Klemperer, J. Appl. Phys. **71**, 3721 (1992).
[8] U. Flender and K. Wiesemann, J. Phys. D **27**, 509 (1994).
[9] A. V. Phelps, J. Appl. Phys. **76**, 747 (1994).
[10] R. T. Farouki, S. Hamaguchi, and M. Dalvie, Phys. Rev. A **44**, 2664 (1991).
[11] D. Wang, T. Ma, and Y. Gong, J. Appl. Phys. **73**, 4171 (1991).
[12] R. M. Chaudrhi and M. L. Oliphant, Proc. R. Soc. London, Ser. A **137**, 662 (1932).
[13] W. D. Davis and T. A. Vanderslice, Phys. Rev. **121**, 219 (1963).
[14] I. Abril, A. Gras-Marti, and J. A. Vallés-Abarca, Phys. Rev. A **28**, 3677 (1983).
[15] J. E. Lawler, Phys. Rev. A **32**, 2977 (1985).
[16] S. Kumar and P. K. Ghosh, Int. J. Mass Spectrom. Ion Processes **127**, 105 (1993).
[17] D. Healy and W. W. Brandt, Int. J. Mass Spectrom. Ion Processes **70**, 267 (1986).
[18] P. P. Ong and M. J. Hogan, J. Phys. B **18**, 1897 (1985).
[19] I. M. Kagan and V. I. Perel, Doklady Akad. Nauk SSSR **98**, 575 (1954) [Sov. Phys. Dokl. **98**, 575 (1954)].
[20] G. H. Wannier, *Statistical Physics* (Wiley, New York, 1966), pp. 462–466.
[21] J. A. Hornbeck and G. H. Wannier, Phys. Rev. **82**, 458 (1951).
[22] T. Makabe and H. Shinada, J. Phys. D **18**, 2385 (1985).
[23] S. L. Lin and J. N. Bardsley, J. Phys. B **8**, L461 (1975).

[24] H. R. Skullerud and S. Holmstrom, J. Phys. D **18**, 2375 (1985).
[25] S. L. Lin and J. N. Bardsley, J. Chem. Phys. **66**, 435 (1977).
[26] J. L. Moruzzi and L. Harrison, Int. J. Mass Spectrom. Ion Phys. **13**, 163 (1974).
[27] H. A. Fhadil, D. Mathur, and J. B. Hasted, J. Phys. B **15**, 1443 (1982).
[28] J. K. Olthoff, R. J. Van Brunt, Y. Wang, R. L. Champion, and L. D. Doverspike, J. Chem. Phys. **91**, 2261 (1989).
[29] D. L. Albritton, I. Dotan, W. Lindinger, M. McFarland, J. Tellinghuisen, and F. C. Fehsenfeld, J. Chem. Phys. **66**, 410 (1977).
[30] H. Mase, T. Tanabe, K. Taneko, and G. Miyamoto, J. Phys. D **12**, L123 (1979).
[31] H. Sugawara, Y. Sakai, and H. Tagashira, J. Phys. D **25**, 1483 (1992).
[32] K. G. Müller and P. Whale, Z. Phys. **179**, 52 (1964).
[33] A. V. Phelps, B. M. Jelenkovic, and L. C. Pitchford, Phys. Rev. A **36**, 5327 (1987).
[34] B. M. Jelenkovic and A. V. Phelps, Phys. Rev. A **36**, 5310 (1987).
[35] J. A. Hornbeck, Phys. Rev. **84**, 615 (1951).
[36] A. V. Phelps and B. M. Jelenkovic, Phys. Rev. A **38**, 2975 (1988).
[37] H. W. Ellis, R. Y. Pai, E. W. McDaniel, E. A. Mason, and L. A. Viehland, Atomic Data Nucl. Data Tables **17**, 177 (1976).
[38] G. H. Wannier, Phys. Rev. **83**, 281 (1951); **87**, 795 (1952).
[39] D. A. Scott and A. V. Phelps, Phys. Rev. A **43**, 3043 (1991).
[40] A. V. Phelps, J. Phys. Chem. Ref. Data **20**, 557 (1991).
[41] J. Fletcher and H. A. Blevin, J. Phys. D **14**, 27 (1981).
[42] A. V. Bondarenko, Zh. Tech. Phys. **43**, 821 (1973) [Sov. Phys. Tech. Phys. **18**, 515 (1973)].
[43] L. J. Kieffer and R. J. Van Brunt, J. Chem. Phys. **46**, 2728 (1967); R. J. Van Brunt and L. J. Kieffer, *ibid.* **63**, 3216 (1975).
[44] K. Köllmann, Int. J. Mass Spectrom. and Ion Phys. **17**, 261 (1975).
[45] S. B. Vrhovac, J. M. Jelenkovic, J. K. Olthoff, and R. J. Van Brunt, *Proceedings of the Tenth International Conference on Gas Discharges and Their Applications, Swansea* (University College of Swansea, Swansea, UK, 1992), pp. 510–512.
[46] W. H. Cramer, J. Chem. Phys. **30**, 641 (1959).
[47] R. Hegerberg, M. T. Elford, and H. R. Skullerud, J. Phys. B **15**, 797 (1982).
[48] R. F. Stebbings, B. R. Turner, and A. C. H. Smith, J. Chem. Phys. **38**, 2277 (1963).
[49] N. Kobayashi, J. Phys. Soc. Jpn. **38**, 519 (1975).
[50] S. B. Vrhovac, S. B. Radovanov, Z. Lj. Petrovic, and B. M. Jelenkovic, J. Phys. D **25**, 217 (1992).
[51] B. N. Klyarfel'd, L. G. Guseva, and Pokrovskaya-Soboleva, Zh. Tech. Phys. **36**, 704 (1966) [Sov. Phys. Tech. Phys. **11**, 520 (1966)].
[52] F. M. Penning and C. C. J. Addink, Physica (Utrecht) **1**, 1007 (1934).
[53] D. Bhasavanich and A. B. Parker, Proc. R. Soc. London Ser. A **358**, 385 (1977).
[54] H. Büttner, Z. Physik **111**, 750 (1939).
[55] R. Schade, Z. Physik **108**, 353 (1938).
[56] V. I. Kolobov and A. Fiala, Phys. Rev. E **50**, 3018 (1994).
[57] Z. Lj. Petrovic and A. V. Phelps, Phys. Rev. E **47**, 2806 (1993); A. V. Phelps, Z. Lj. Petrovic, and B. M. Jelenkovic, *ibid.* **47**, 2825 (1993).
[58] F. Howorka, W. Lindinger, and R. N. Varney, J. Chem. Phys. **61**, 1180 (1974).
[59] M. M. Shahin, J. Chem. Phys. **47**, 4392 (1967).
[60] R. C. Bolden, S. P. Jeffs, and N. D. Twiddy, Chem. Phys. Lett. **23**, 73 (1973).
[61] R. J. Van Brunt and J. K. Olthoff, *Proceedings of the 8th International Seminar on Electron and Ion Swarms, University of Trondheim* (NTH, Trondheim, Norway, 1993), pp. 76–78.
[62] R. Johnsen, A. Chen, and M. A. Biondi, J. Chem. Phys. **73**, 1717 (1980).
[63] M. Grössl, M. Langenwalter, H. Helm, and T. D. Märk, J. Chem. Phys. **74**, 1728 (1981).
[64] T. Holstein, J. Phys. Chem. **56**, 832 (1952).
[65] D. Rupp and W. E. Francis, J. Chem. Phys. **37**, 2631 (1962).
[66] H. Helm, J. Phys. B **10**, 3683 (1977).
[67] R. Johnson, J. Phys. B **3**, 539 (1970).
[68] C.-L. Liao, X.-X. Liao, and C. Ng, J. Chem. Phys. **82**, 5489 (1985).
[69] K. McAfee, W. Falconer, R. Hozack, and D. McClure, Phys. Rev. A **21**, 827 (1980).
[70] M. L. Vestal, C. R. Blakely, and J. H. Futrell, Phys. Rev. A **17**, 1337 (1978).
[71] W. Aberth and D. C. Lorents, Phys. Rev. **144**, 109 (1966).
[72] S. Vrhovac, S. Radovanov, Z. Petrovic, and B. Jelenkovic, *Program and Abstracts of Papers of the Joint Symposium on Electron and Ion Swarms and Low Energy Electron Scattering* (Bond University, Gold Coast, Queensland, Australia, 1991), pp. 80–82.